Scientific Research Publishing

Open Journal of Geology, 2024, 14, 1016-1037
https://www.scirp.org/journal/ojg
ISSN Online: 2161-7589
ISSN Print: 2161-7570

Structural Controls of the Coastal Bujuru and Retiro Heavy Minerals Deposits in Southern Brazil

Bruno Silva da Fontoura[1], Adelir José Strieder[2*], Iran Carlos Stalliviere Corrêa[1], Paulo Rogério Mendes[3], Aureliano V. Nóbrega[4]

[1]Programa de Pós-graduação em Geociências (PPGeo), Instituto de Geociências, UFRGS, Porto Alegre, Rio Grande do Sul, Brazil
[2]STR Data & Geologia Ltda., Rua Pedro Thorstenberg 283, Ijuí, Rio Grande do Sul, Brasil
[3]HIDROSERV—Serviços Geológicos e Geofísicos Ltda., Rua Senegal 152, Porto Alegre, Rio Grande do Sul, Brazil
[4]Rio Grande Mineração S.A., Rua Borges de Medeiros, 168, Bairro Centro, São José do Norte, Rio Grande do Sul, Brazil
Email: *adelirstrieder@outlook.com

How to cite this paper: da Fontoura, B.S., Strieder, A.J., Corrêa, I.C.S., Mendes, P.R. and Nóbrega, A.V. (2024) Structural Controls of the Coastal Bujuru and Retiro Heavy Minerals Deposits in Southern Brazil. *Open Journal of Geology*, **14**, 1016-1037.
https://doi.org/10.4236/ojg.2024.1412045

Received: October 16, 2024
Accepted: December 7, 2024
Published: December 10, 2024

Abstract

This paper shows new results for Bujuru and Retiro HM deposits geological control, located in the Coastal Plain of the Rio Grande do Sul state (Brazil). Ground Penetrating Radar (GPR), drillholes and fieldwork were applied to investigate deformational structures that control Holocene sediment deposition and the HM deposits accumulation. The Bujuru and Retiro HM deposits were developed as a consequence to deformational traps (synthetic and antithetic normal faults). Mechanical subsidence and hanging-wall rotation, instead of sea level changes, are the main controlling mechanism for structural placers development that leads to existing HM deposits. Based on listric fault displacement and sedimentation rates, it is possible to distinguish three stages of lagoonal deposition, and two main episodes of HM accumulation. The preliminary HM concentration episode is due to sediment reworking from Pleistocene footwall escarpment and from a Pleistocene structural barrier developed in the hanging-wall oceanward (LFS 6). The second HM concentration episode is characterized by TDS and TD (LFS 5) developing upon a brachyanticline built due to the progressive deformation of the hanging-wall that includes previous Holocene lagoonal radarfacies. The TDS and TD are a sedimentary barrier and migrate inland due to NE onshore winds that also accumulate over the structurally controlled lagoons.

Keywords

HM Placer Deposits, Gravity-Driven Deformation, Structural Traps

1. Introduction

Detrital heavy mineral (HM) deposits are significant in several countries, such as Vietnam, Australia, the United States and Brazil. Despite ilmenite is largely the most abundant mineral; some others may show a concentration such that it can make this type of ore deposits to be even more economic.

The HM placer deposits in coastal plains tend to have their evolution controlled by sea level changes; by weathering, erosion, and reworking of sedimentary rocks and coastal sediments; by sediment deposition from offshore to backshore; or by aeolian erosion and deposition in dunes ridges (e.g. [1]-[5]). In this way, HM deposits along southern Australia, west Africa and southern Vietnam coast seem to display similar characteristics to Bujuru HM deposits in Rio Grande do Sul Coastal Plain (RGSCP, southern Brazil; [6]).

Along the South America Atlantic Coast, there exist several HM occurrences hosted in Holocene beach sediments (e.g. [3] [4] [7]-[14]). However, only two of them showed mean HM concentration up to 4.5% to be mined: i) Guaju Mine in Mataraca (Paraíba state; [15]), and ii) Bujuru and Retiro areas (Rio Grande do Sul state, [16]).

Most studies are focused on the transport and deposition of HM (e.g. [17]-[20]) to build up an economic deposit (e.g. [1] [21]) on coastal plains. The recent advances investigate aeolian landforms that can develop aeolian mineral deposits [22], and summarize sedimentological parameters, mineralogical and chemical compositions for different landforms series to be used as prospective proxy ([23] [24]).

The investigations on Brazilian Atlantic coast HM occurrences consider a scenario where coastal units are dynamically homogeneous, at least during upper Holocene (<8000 yr BP). However, recent investigations on central Rio Grande do Sul Coastal Plain (RGSCP) revealed a large-scale growth fault controlling sedimentation in Bujuru District area [25].

The aim of this paper is to present the deformational framework that controls the placing of Bujuru to Retiro HM deposits in the RGSCP during the Holocene. 50 MHz RTA Ramac GPR surveys, drillholes and field surveys were carried out to investigate the regional deep structures, as well as recent dunes barrier encompassing HM concentrations. Some GPR surveys in RGSCP were conducted by some researchers (e.g. [6] [26] [27]), but they are focused on sedimentary features of upper strata, and do not search for deep deformational structures.

2. Geological Setting

The Rio Grande do Sul Coastal Plain (RGSCP) is the emerged part of the Pelotas Basin, which started deposition in the Barremian/Aptian (125 Ma approximately), after Gondwana rupture. The coastal plain is up to 100 km wide and >600 km long. The geomorphic and stratigraphic configuration of RGSCP is currently described to be formed by deltaic alluvial plains and four lagoons/barrier systems in response to sea level changes between Middle Pleistocene and Holocene eras (**Figure 1**).

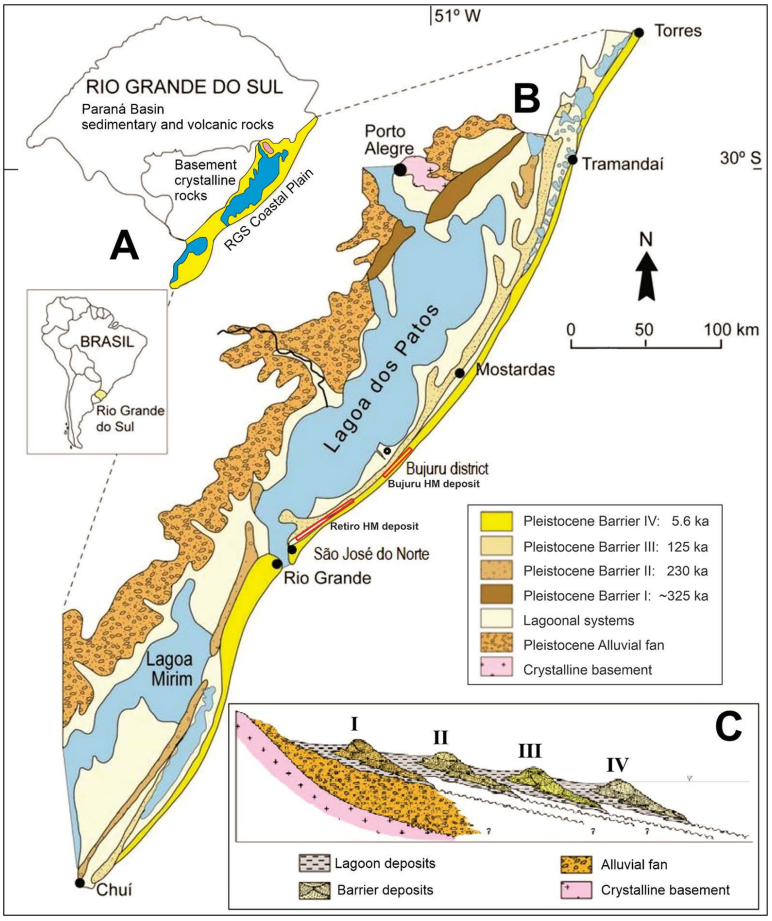

Figure 1. Rio Grande do Sul Coastal Plain location (A), its reginal geological map and HM deposits placement (B), and the model for its depositional systems (C). Modified from [28] and [29]. Lagoon/Barrier system ages according to [30].

São José do Norte County (RS, Brazil) presents two HM placer deposits, which is now under licensing for mining: i) Bujuru and ii) Retiro. Both make up the largest known deposit in Brazil, and display similar structural, sedimentological, mineralogical, and economic grade characteristics [6] [16] [31].

According to [6], the Bujuru deposit is closely related to the sediments deposited by the old Camaquã River course, whose position at 125 ka was geographically close to the present deposit. Similar heavy mineral content was identified in surface sediments from the adjacent shield [32]-[34].

Dillenburg *et al.* [6] proposed a three-step scenario for Bujuru HM deposit formation. The first step incorporated HM into the beach and wash over facies of a transgressive barrier during the Postglacial Marine Transgression (ends at 5.6 ka). The second step additionally concentrated HM in backshore deposits by eroding and recycling Pleistocene sediments during slow sea-level fall and Holocene barrier retreat. And, the third step eroded backshore deposits and HM was transported by onshore winds into an inter-barrier depression to give rise to transgressive dune deposits.

Fontoura *et al.* [25] investigations showed that the inter-barrier depression in

the Bujuru area is, in fact, due to a large, gravity-driven listric growth fault, which controls the Lagoa do Peixe escarpment and hanging-wall sedimentation. [25] also showed that the balance of fault displacement and sedimentation rates established three main radarfacies (Figure 2). Table 1 summarizes the main findings related to the Lagoa do Peixe Growth Fault displacement and sedimentation.

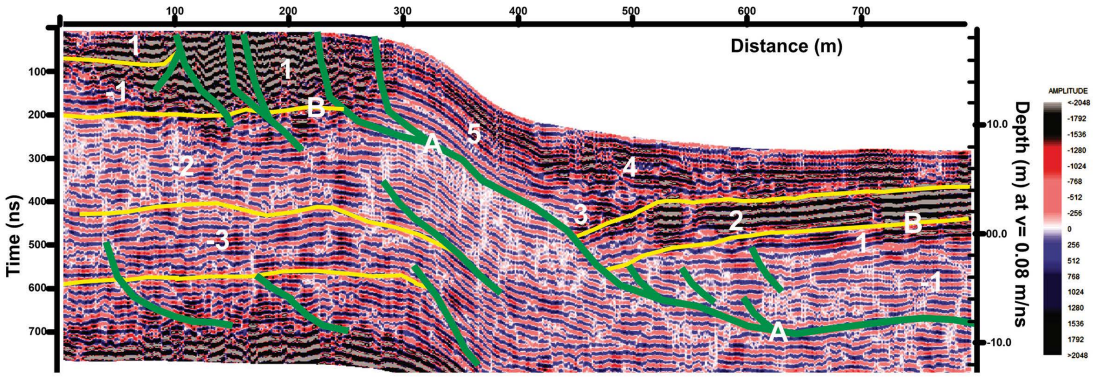

Figure 2. Radargram in the Talhamar Road (Tavares, Brazil), cutting across Lagoa do Peixe Growth Fault (Tavares GPR line 2). See Table 1 for a description of the geophysical units and surfaces.

Table 1. Summary of main radar radarfacies and surfaces distinguished for GPR survey lines in the Lagoa do Peixe and Bujuru HM deposit (RGSCP, Brazil). See [25] for a detailed description and analysis.

Radarfacies/Surface	DESCRIPTION
−1, −2, −3	Pleistocene sedimentary (geophysical) units that do not crop out in the area of investigation.
1	Pleistocene sediments cropping out at the footwall top west of fault escarpment (Barrier III).
A	Upward concave geometry surface that truncate Pleistocene sediments (west) and lower lagoonal unit (east): Listric gravitational growth fault.
B	*Offlap-toplap* for reflectors underlying lower lagoonal unit: an erosional surface developed on the down-throwing hanging-wall before fault controlled lagoonal accumulation.
2	Convex upward arcuted lower lagoonal unit, displaying *onlap* for lowermost reflections in the thickest zones (2a), close to listric surface, and parallel reflections (2b) for uppermost strata. The upper sediments of this radarfacies are aged 3.49 ka (Dillenburg *et al.* 2004) **First stage**: fault displacement rate higher than sedimentation rate.
3	Horizontal reflections in a hanging-wall triangular area close to listric surface, showing *onlap* upon lower lagoonal unit and listric surface. **Second stage**: equalized fault displacement and sedimentation rates.
4	Upward arcuated reflections at both Lagoa do Peixe margins, showing alternating *onlap-downlap* and *toplap-offlap* features. The peat layer cropping out at Bujuru District is aged 1.06 ka (Dillenburg *et al.* 2004) and is defined as the lowermost strata of this radarfacies. **Third stage**: sedimentation rate higher than fault displacement rate.
5	Dipping sinuous reflections in the Lagoa do Peixe escarpment, showing discrete downlap with lagoon sediment reflections. Erosional degradation of the fault escarpment and deposition as interbedded layer of sands and lagoon sediments.

Continued

C	Irregular surface underlying recent dune sediments. Surface upon which recent dune sediments are laid on with down lapping features (6a).
6	Horizontal and steeply dipping sigmoidal reflections (6a), as also as thin horizontal reflection (6b) near the topographic surface, produced by Holocene transgressive dunes and dune sheets.

3. Geological and Geophysical Surveying Methods

Satellite images and aerial photographs were applied to investigate local and regional geological and sedimentary features. They enabled to recognize the fault escarpment to the northwest lagoon borders, and to delineate the Holocene transgressive dunes and dune sheets (TD and TDS) due to southwest direct onshore winds. They also enabled to identify the continuity of surficial sedimentary units during field works.

The GPR survey lines were acquired perpendicular to shoreline, to the fault escarpment and to TD direction (Figure 3). Some challenges were faced in setting GPR acquisition parameters (frequency, depth of penetration, sampling frequency). But the main challenges were regarded to data processing, since mandatory procedures must be precisely adjusted to avoid geophysical artifacts and reinforce structural and geological features.

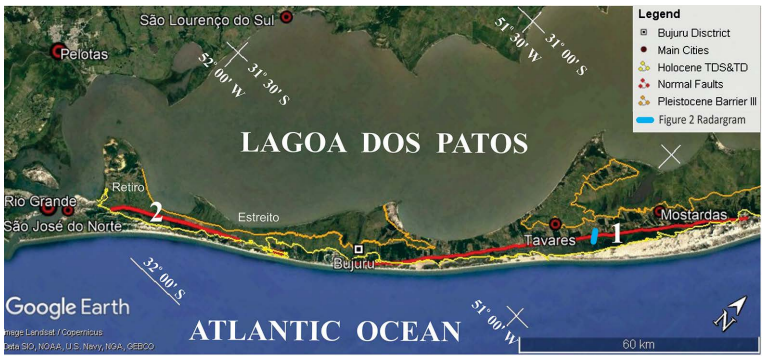

Figure 3. Simplified geological map of the Retiro and Bujuru HM deposits area, showing the tip zone of the Lagoa do Peixe (1) and Retiro-Estreito (2) faults.

The GPR surveys were produced mainly by a 50 MHz (RTA) antenna, and the acquired using Pro-EX GPR System (MALA-RAMAC). Acquisition parameters were set to high lateral resolution (20 cm trace spacing) and time window to investigate at least 20 - 23 m depth. The mean vertical resolution was determined through hyperbola analysis on radargrams. The first geophysical campaign used a minor time window, and the velocity was approximated to 0.09 m/ns (vertical resolution close to 0.9 m); the second campaign used a greater time window, and the mean velocity was approximated to 0.08 m/ns (vertical resolution close to 0.8 m).

The GPR survey lines were tracked by DGPS (Emlid, Reach RS + model, base and rover receptors). The kinematic and post-processed corrections (PPP-IBGE and Leica Geo Office, respectively) do permit a high horizontal (7 mm + 1 ppm)

and vertical precisions (14 mm + 1 ppm) positioning.

Post-processing used Reflex-W software and included the following main steps: dewow filter; bandpass filter (butterworth, but sometimes trapezoidal); migration (v = 0.297 m/ns) for removing surface reflections in unshielded antenna; topographic correction; 3D topographic migration (e.g. v = 0.08 m/ns) and butterworth filtering.

Three percussion cores were drilled to correlate with GPR survey line (Bujuru 01). This GPR survey line extends to the beach, and the drillholes were set in it to follow the peat layer cropping out in the beach. Then, it was possible to determine the sand thickness covering the peat layer, and the stratigraphic features of the Pleistocene barrier (III) sediments.

4. Structural and Geologic Controls of HM Deposits

Satellite images and aerial photographs interpretation and fieldwork made it possible to distinguish between main geological features and structures. As pointed out by [25], the northwest margin of the Lagoa do Peixe (lagoon) is controlled by a listric growth fault (**Figure 2**), whose displacement gave rise to mechanical subsidence for lagoonal sedimentation.

Bujuru HM deposit is located at the southwestern tip of the Lagoa do Peixe Growth Fault. The Bujuru area is also de tip zone for the Retiro-Estreito Fault (**Figure 3**), which controls the northwest margin of another almost clogged lagoon located to the southwest. This tip zone for both, Lagoa do Peixe and Retiro-Estreito faults (**Figure 4(A)**), is a structurally elevated area, where lower sedimentary units are exposed due to the rotation during listric fault displacement.

The tip zone for both Lagoa do Peixe and Retiro-Estreito faults is entirely covered by Holocene transgressive dunes (TD) and dune sheets (TDS), which extends well upon Pleistocene sediments (Barrier III). In this area, then, one cannot yet exactly define the faults interactions and fault-controlled sedimentation.

Retiro HM deposit, on the other hand, extends from midway through the southwest tip of the Retiro-Estreito Fault (**Figure 4(B)**). The Holocene TD and TDS cover the fault tip zone close to São José do Norte city, so that it also cannot yet be exactly followed.

The recent sedimentation process in the fault-controlled lagoons has taken place under very low fault displacement rate (Stage 3, **Table 1**). **Figure 5** and **Figure 6** show the geomorphic expression of two sedimentary processes that are actually

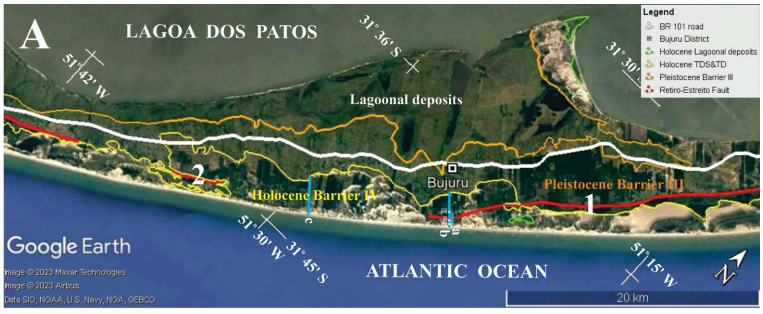

Figure 4. Simplified geological map for Bujuru (A) and Retiro (B) HM deposits. Lagoa do Peixe (1) and Retiro-Estreito (2) normal fault traces define the Northwest escarpment against Pleistocene sediments. Legend GPR radargrams: a) **Figure 9** radargram; b) **Figure 10** radargram; c) **Figure 11** radargram. i-iii: boreholes locations in the Bujuru area.

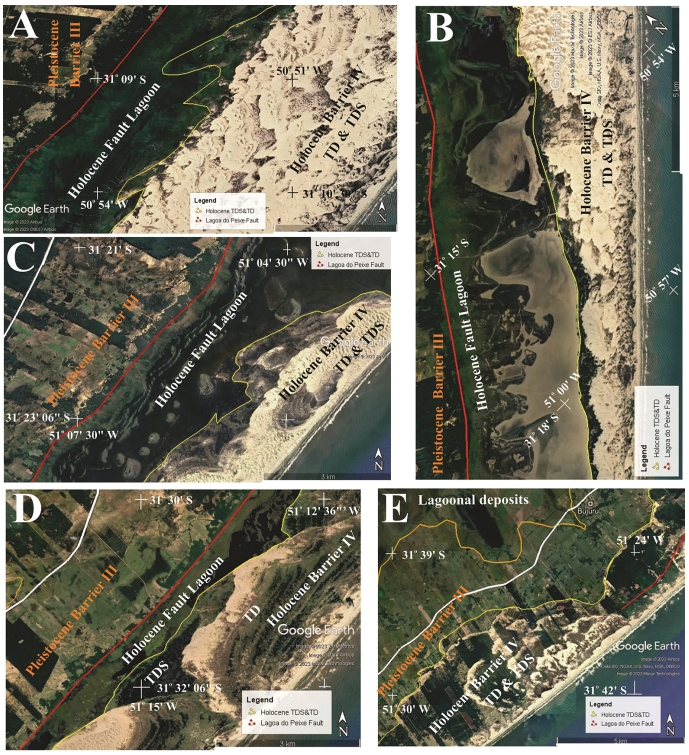

Figure 5. High resolution Google satellite images in the Lagoa do Peixe area from north (A) to south (E) showing the interplay of two clogging processes, from aeolian dunes construction (A), to gravity- and hydraulic-driven deposition (B), a combination of both (C), and the final fill of the lagoon by aeolian dunes (D, E).

clogging both lagoons: i) erosion of previous stage lagoonal sediments in fore to backshore, and onshore wind transport (NE to SW) in the hinge zone of the rotating hanging-wall fault block (**Figure 5(A)**, **Figure 5(C)**, **Figure 5(D)**, **Figure 5(E)** and **Figure 6(A)**, **Figure 6(B)**); ii) fault scarp erosion and gravity- and hydraulic-driven transport into de lagoon (**Figure 5(B)**, **Figure 5(C)** and **Figure 6(A)**).

Along the Retiro-Estreito Fault (Figure 6), some of these sedimentary processes can also be observed. However, the TD and TDS cover almost completely the original lagoon. On the other hand, Retiro-Estreito Fault has half the Lagoa do Peixe Growth Fault trace length. Then, it is to be expected that vertical fault displacement should be proportionally less. In a recent evaluation, it is observed that there is a larger predominance of aeolian process upon this lagoon.

In the structural high developed at the tip zone for both Lagoa do Peixe and Retiro-Estreito faults (Figure 5(E)), the peat layer defining the base of the upper depositional radarfacies (1.06 ka, Figure 7(A)) is under wave erosion and dispersion along the beach. The TD and TDS cover discordantly the exposed peat layer (Figure 7(B)). These fragments are being covered by aeolian sediments and being incorporated into interdune layers (Figure 7(C), Figure 7(D)).

The base of dunes and interdune space are also the main locus for HM accumulation, where it displays a horizontal stratification (Figure 7(E), Figure 7(F)).

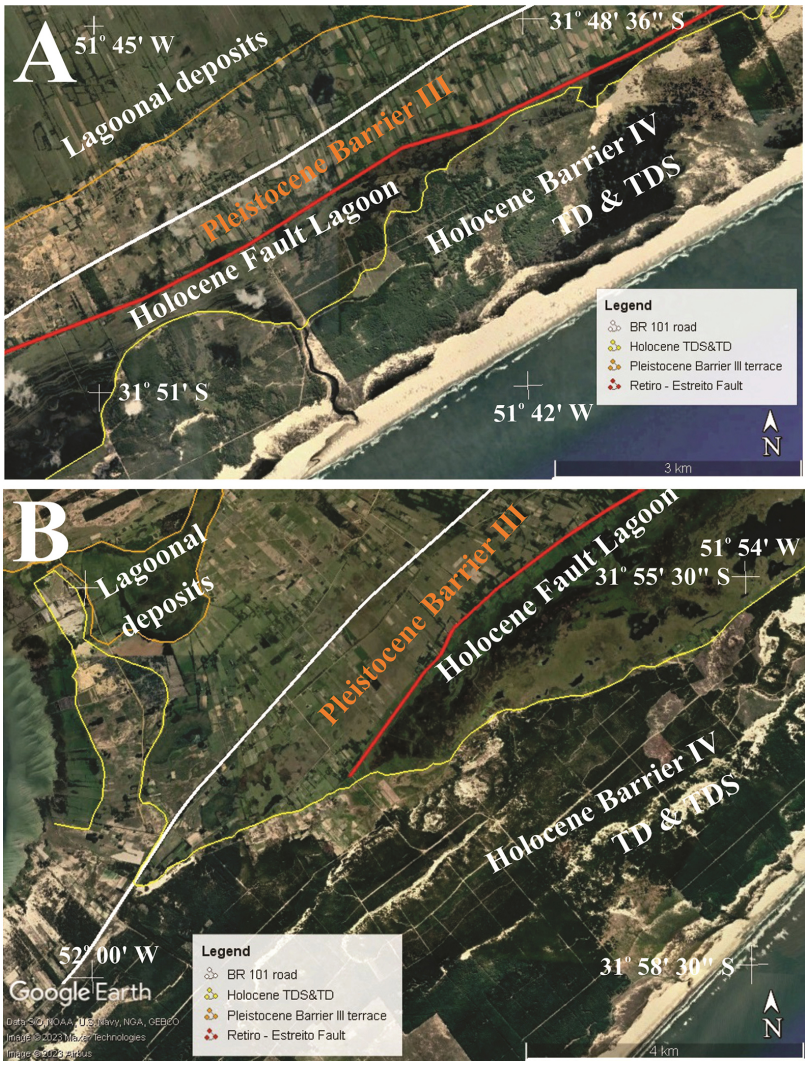

Figure 6. High resolution Google satellite images in the Retiro (A) and Estreito (B) showing the predominance of aeolian dunes construction in these areas.

Figure 7. Stratigraphic relationships between peat layer and TD hosting HM in the structural high at Bujuru District. A) Peat layer cropping out ate Bujuru beach under erosional fragmentation. B) Undulated contact between peat and dune sediments. C) Vertical peat fragment identified in a excavated trench. D) Horizontal peat fragment in an excavated trench. E) Natural vertical cut of HM layering close to interdune area. F) Orthogonal trench cut showing HM lamination; note higher HM concentration in the horizontal layering.

5. Geophysical Structures Controlling HM Deposits

GPR lines were surveyed in the NW-SE direction to investigate the NW dipping peat layer (Radarfacies 3) and the underlying lagoonal sediments (Radarfacies 1). This direction is also perpendicular to gravitational faults. Then, GPR surveying was conducted to emphasize the deformational structures and their relationships with TD deposition. In this direction, it is to be noted that TD stratification will appear as two different geophysical signatures: i) dipping sigmoidal reflections for the lateral segment (6a) of TD, and ii) thin horizontal reflection (6b) for the frontal segment of TD (see Table 1).

The geological control of upper radarfacies was carried out based on surface geologic surveying and based on three percussion drills located midway between GPR lines Bujuru-2 and PB-13 (a and b in Figure 4). The drillhole logs are presented in Figure 8, and show the Pleistocene sediments (radarfacies 1), the peat layer cropping out in Bujuru beach (base of the radarfacies 4), and Holocene TD

and TDS (radarfacies 6a and 6b).

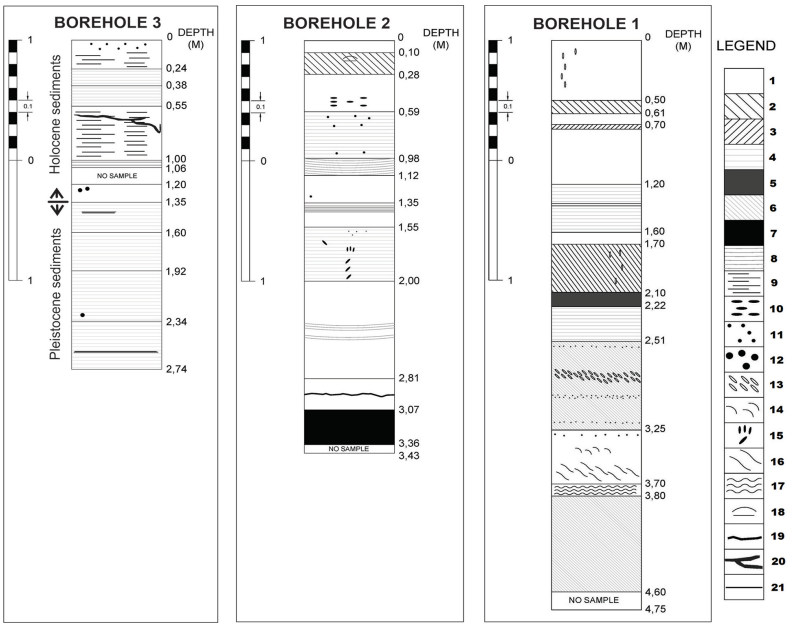

Figure 8. Description of the percussion Drillholes Logs in the Bujuru area. Borehole logs legend: 1) Light yellow sand; 2) Light yellow sand with coarse lamination (1 - 5 mm thick); 3) light yellow sand with gently inclined lamination (1 - 2 mm thick) and disseminated heavy minerals; 4) light yellow sand with thin horizontal lamination (1 mm) and disseminated heavy minerals; 5) Massive, dark gray sand with high quantity of heavy minerals; 6) Massive light yellow sand and disseminated heavy minerals; 7) Peat; 8) light yellow sand with gently arched lamination (1 mm); 9) isolated thin horizontal laminas of heavy minerals; 10) up to 2 cm recent root fragments; 11) small recent root fragments; 12) small disseminated shell fragments; 13) up to 1 cm shell fragments; 14) oxidized material; 15) oxidized (orange) dark gray sand; 16) heavy minerals concentration; 17) light yellow sand with fragmentary structure; 18) dispersed organic matter; 19) relicts of organic matter; 20) local breccia structure; 21) dark yellow sand lamination.

Figure 9 shows a radargram surveyed for the deepest structural relationships in the Bujuru HM deposit area. It emphasizes the normal fault truncation of the Pleistocene units (1), and the first (2) and third (4) lagoonal radarfacies. The transgressive nature of the Holocene dunes (6) can be recognized by their both lateral and frontal geophysical signatures.

Two other GPR lines were selected to illustrate the deformational structures, and the sedimentary relationships between each radarfacies. Such GPR lines were located close to Bujuru Project drillhole sections, to better correlate direct data with geophysical results (PB-01 and PB-13). In this way, a re-interpreted profile is presented with each of the radargrams (**Figure 10(B)** and **Figure 11(B)**).

Figure 10(A) shows the radargram close to PB-13 drillhole section, which is also parallel and close to radargram present in **Figure 9** (~500 m to the NE). The most striking geological feature is the presence of two normal faults dipping towards the SE. The peat layer overlying the first lagoonal radarfacies (2b) is

interrupted in the hanging-wall block, as already noticed in Figure 2.

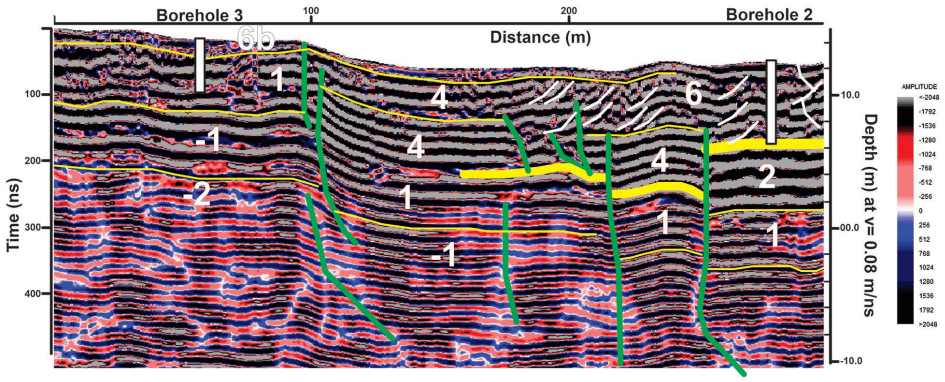

Figure 9. Radargram depicting deep structural relationships in the Bujuru area. Radargram legend: i) white numbers: radarfacies as presented in Table 1; ii) green lines: normal faults; iii) thick yellow lines: ~1.0 m peat layer cropping out at Bujuru beach; thin yellow lines: geophysical units/radarfacies; white lines: lateral stratification of dunes (6a in Table 1). Boreholes position is projected into the radargram.

The first lagoonal radarfacies (2), then, is folded to a gentle synclinal and an anticlinal in the hanging-wall block (Figure 10(A)), due to normal, listric faulting. It can be recognized that the thickest TD is deposited in the synclinal, where the lateral geophysical signature of TD (6a) shows its best downlap expression over the exposed peat layer (C). Fieldwork has also observed that gentle folds are, in fact, brachyanticlines and brachysynclines, since their hinge zone dips NE and SW parallel to the master listric normal faults.

The PB-13 radargram (Figure 10(A)) also enabled to distinguish two different first lagoonal radarfacies (2a and 2b) overlying the Pleistocene sediments (1). They correspond well to PB-13 Drillhole Section description (Figure 10(B)). The Drillhole section can be re-interpreted based on radargram by including fault displacement of some key sedimentary strata.

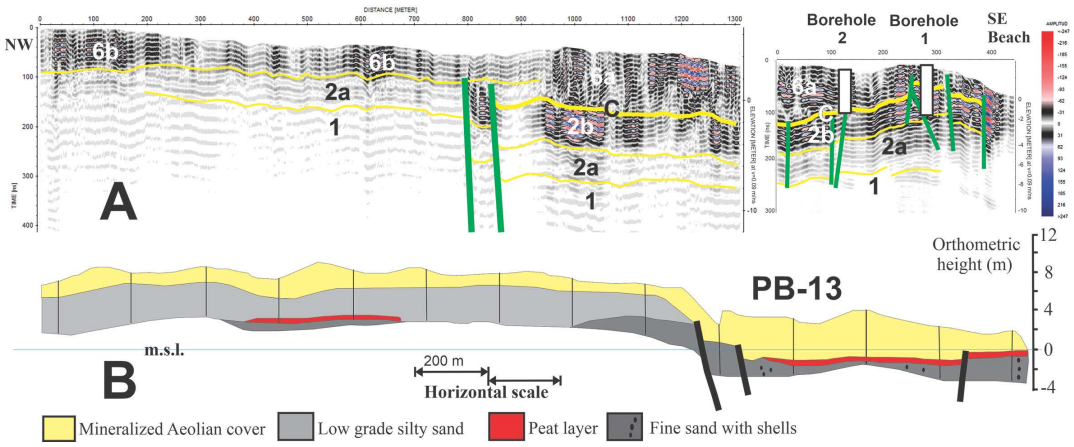

Figure 10. PB-13 section structural features. A) Radargram close to B) PB-13 drillhole section. Drillhole section under permission of RGM S.A. Radargram legend as shown in Figure 9.

Figure 11(A) is a radargram surveyed to the southwest (~11 km SW of PB-13), near to PB-01 Drillhole Section, midway between Lagoa do Peixe and Retiro-Estreito faults exposed tips. It shows mainly the gentle anticline close to the beach, and the first half of the synclinal. PB-01 radargram presents quite the same radarfacies as described for Figure 10(A). However, an additional radarfacies was distinguished: the third lagoonal one (4, as described in Table 1), onlapping the first lagoonal one (2). It is to be noticed that peat layer cropping out at Bujuru beach is one of the basal strata of the third lagoonal radarfacies (4).

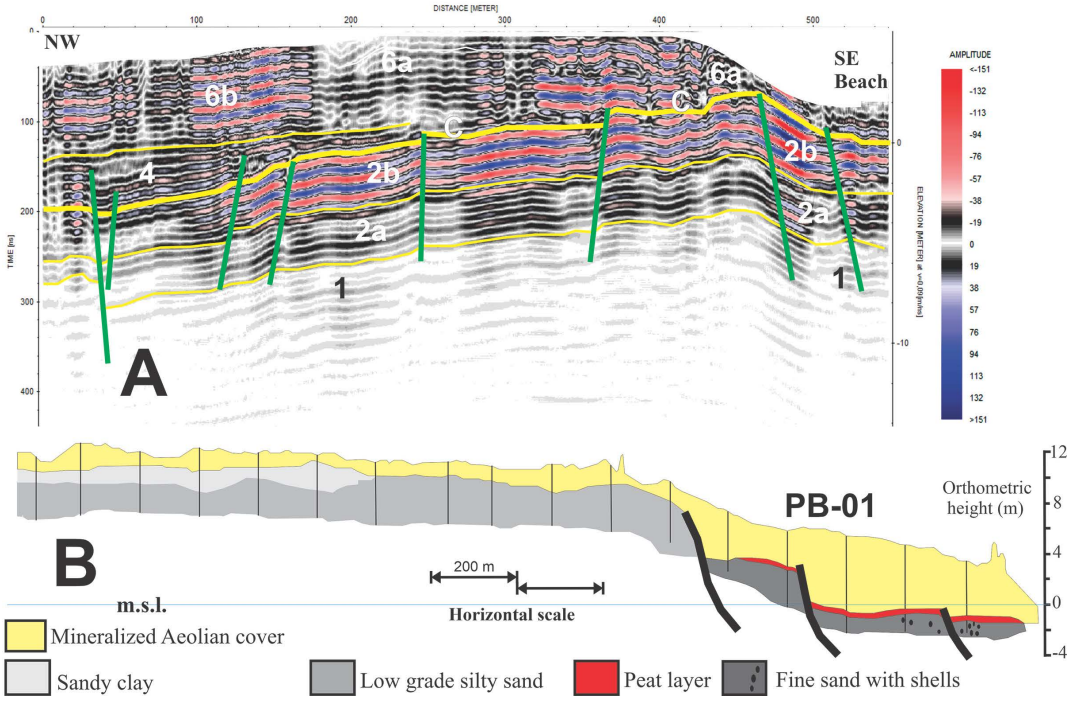

Figure 11. PB-01 section structural features. A) Radargram close to B) PB-01 drillhole section. Drillhole section under permission of RGM S.A. Radargram legend as shown in Figure 9.

Figure 11(B) shows the complete PB-01 Drillhole Section re-interpreted, now including normal listric faults displacing the key layers. The corresponding GPR line was placed some distance to the north due to access facilities and represents just the ~600 m of its southeastern segment. In any way, the correlation between radargram and drillhole section is quite good.

6. Discussion

Deep GPR surveys in the Bujuru and Retiro HM deposits brought in evidence of a series of deformational structures that were not yet described for the RGSCP: listric normal faults related to gravitational tectonic supported by the exposed segment of the Pelotas Basin.

Radargrams presented in Figure 2, Figure 9, Figure 10 and Figure 11 show the main deformational structures controlling the erosional and depositional conditions supported by the RGSCP from the onset of faulting. The onset of gravitational

tectonics in the Bujuru District is estimated to be 9 - 8 ka taken the geological records for lagoonal sediments (see [25] [35] for discussion).

The main listric normal faults related to gravitational tectonics promote the hanging-wall block rotation and gentle folding of the stratigraphic units, as also as minor interconnected faults, even synthetic or antithetic ones [36].

The Bujuru HM deposit is placed upon the tip zone of the Lagoa do Peixe and Retiro-Estreito faults (**Figure 4**). Radargrams in this area (**Figures 10-11**) show a gentle anticlinal close to the Bujuru beach, which amplifies toward Retiro-Estreito Fault and gave rise to the hinge zone of the rotating hanging-wall block. That radargrams also show that the thickest Holocene mineralized TD and TDS are placed in the synclinal area. The Retiro HM deposit, on the other hand, is placed mainly upon the depocenter of the fault controlling Retiro Lagoon (hangingwall), and upon the southwestern Pleistocene footwall bulkhead block.

The intersection of two master fault systems at Bujuru District area introduces additional structural complexity in erosion and sedimentary deposition of Holocene radarfacies. Additional investigation is being conducted in this area, since the deformational structures are covered by mineralized Holocene TD and TDS. The extent the down warping block open space for Holocene deposition and erosion of the Pleistocene sediments on the footwall and in the hanging-wall is still under concern. The tip zone of listric faults is also the locus for the development of transfer faults, which introduces additional displacement patterns in the down warping hangingwall and in sedimentary processes and thickness. The presence of some different radarfacies shown in **Figure 9**, **Figure 10** and **Figure 11** is a clear consequence of the diachronous development of regional master and local faults of each interconnecting system.

The HMs are still being transported by onshore winds and deposited in TD (**Figure 7**). It is interesting to observe, however, that HMs are present in the TD overlying exposed peat layer (base of the radarfacies 4) and the underlying radarfacies 2. But, from the northeastern tip zone of Lagoa do Peixe Growth Fault to southwestern exposed tip of the Retiro-Estreito Fault, it is to be noticed that TD and TDS have not HMs, or have very low HM concentration when peat layer is not still exposed due to folding and/or faulting along the beach.

The deformational structures along the fault direction seem to control not only the lagoonal sedimentation (radarfaceis 2 and 4, mainly), but also their erosion to give rise the economic HM deposits. The source for HMs transport by onshore winds and their deposits in Holocene TD is to be considered.

[22] analysed a series quaternary aeolian landforms and the physical, chemical and sedimentological conditions that make possible the development of aeolian mineral deposits of economic grade. [24] reviewed several aeolian landforms with emphasis on their textural, compositional, and geodynamic maturity of the sedimentary deposits, to propose a "hybrid manual" for practical field studies of aeolian mineral deposits. On this basis and on additional research papers, it is possible to evaluate the source and concentration processes that led to Bujuru and

Retiro HM deposits.

The HM occurrences in the RGSCP were first reported by [11] and [37]. Both papers sampled HM in the foreshore and backshore of actual beaches, and suggested the HM were transported by SW to NE swell action. [37] suggested HMs were concentrated by swash and backwash action in the foreshore and backshore, water sheet flows by berm-top spillover and aeolian winnowing action. [37] investigation was restricted to southern RGSCP segment (Cassino to Chuí beaches) and found that the north part has a slight non-opaque minerals predominance, while the south part (Chuí) has opaque minerals predominance.

The proportion of different HMs along RGSCP Holocene beach zones and continental shelf varies. [38] sampled a large area in the continental shelf from north Rio Grande do Sul (Brazil) to north Argentina, to discuss the regional and local sources of HMs based on opaque HMs concentration, and on mineralogical index and multivariate data analysis (non-opaque HMs). [38] showed the higher opaque minerals (ilmenite, limonite, leucoxene e pyrite) concentration in front of Rio de la Plata Estuary, and suggested that it represents a regional source due Rio de la Plata draining mainly Paraná Basin sedimentary and volcanic rocks. Local sources are put in evidence, since non-opaque minerals (hyperstene, hornblende, tourmaline, staurolite, apatite and zircon). [39] showed a large variation on HMs composition from Chuí area to Lagoa da Ave (SC state, to the north), sampled on swash zone, and pointed out some proximal source correlation.

[33] made a series of microprobe analysis in non-opaque HMs along the northern RGSCP and compared their chemical composition with composition of same minerals from different stratigraphic units: continental plateau basalts (Serra Geral Fm., Paraná Basin) and Rio Grande do Sul Precambrian Shield (granite-gneisses and metamorphosed vulcano-sedimentary rocks). [33] found that non-opaque HMs are mainly derived from RGS Precambrian Shield. Additionally, [34] analysed zircon composition and found that zircon grains mainly derived from an association of subalkaline to alkaline granitic rocks of nearby Pelotas Batholith (RGS Precambrian Shield). These results corroborate [38] results for HM sampled in the continental shelf.

The sediment reworking in the RGSCP is usually mentioned as a mechanism for HMs differentiation and concentration. [40] sampled different barrier/lagoon system near Chuí area (southmost area of RGSCP) and showed some different HMs concentrations in each barrier/lagoon system. Additionally, [40] reported an increase in total concentration of HMs from Barrier/Lagoon II to Barrier/Lagoon IV (0.042%; 1.89%; up to 4.66%). [41] sampled the aeolian and the upper shoreface-foreshore facies for all four Barrier/Lagoon systems and could define some trends for HMs differentiation from older to younger barrier/lagoon systems. However, [40] and [41] investigations have limited sampling locus distribution in the RGSCP for a complete discussion about HMs differentiation along barrier/lagoon systems.

Table 2 lists HMs compositional differentiation and concentration determined in some of previous investigations to compare them with Bujuru and Retiro HM

deposits. It is noteworthy that ilmenite + magnetite is the most abundant HM specie in each barrier/lagoon system, and sampling site. It is also interesting to observe the expressive epidote + zircon + amphibole + pyroxene increasing from older to younger barrier/lagoon system. This non-opaque HMs increase can imply the advance of Rio Grande Arc denudation processes toward the NNW, where metavolcanic rocks (epidote + amphibole), alkaline granites (zircon) and stratiform mafic-ultramafic complexes (pyroxenes) predominates in the exposed RGS Precambrian Shield.

Bujuru and Retiro HM deposits, in this way, as also [37] and [38] results for backshore-foreshore and shoreface-offshore zones, do reflect these conditions. [38] identified an opaque HM and ZTR anomalous area offshore the Bujuru and Retiro HM deposits.

Table 2. HMs compositional differentiation and concentration as recorded in some investigations to compare with Bujuru and Retiro HM deposits. SKA = sillimanite + kyanite + andalusite.

Barrier/Lagoon System (age)	[37] Hermenegildo-Chuí (southern RGSCP)	[38]	[41] HMs listed in order of abundance	[6] [16] **Bujuru HM deposit**	[31] **Retiro HM deposit**
B/L system IV (8 a 0 ka)	Ilmenite (46.6%), magnetite (3.2%), epidote (10.8%), pyroxene (12.5%), tourmaline (2.6%), staurolite (4.4%), zircon (2.9%), rutile (1.8%), garnet (3.0%), kyanite (1.7%), andalusite (0.3%) and others (9.9%)	Opaque minerals (31.6%): ilmenite, limonite, leucoxene and pyrite. Non-opaque minerals: tourmaline (11.5%), hornblende (9.3%), staurolite (9.3%), augite (8.9%), epidote (7.4%), hypersthene (6.3%), zircon (4.5%), garnet (4.4%), kyanite (3.9%), apatite (3.6%), sillimanite (1.1%) and rutile (0.8%)	Ilmenite + magnetite, epidote, zircon, rutile, tourmaline, staurolite, garnet, SKA, amphibole, pyroxene, chromite + pinels	Ilmenite (58.6%), zircon (8.4%), epidote (8%), tourmaline (6.3%), magnetite (5.3%), staurolite (5%), rutile (2.5%), kyanite (2.1%), leucoxene (2.1%), garnet (0.7%), perovskite (0.5%), chromite (0.3%) and others (0.2%)	Ilmenite (62.3%), zirconite (7.5%), Ti-magnetite (6.2%), quartz (5.9%), epidote (5.2%), staurolite (4.8%), Rutile (2.2%), Turmaline (2.2%), Garnet (1.7%), kyanite (1.1%), leucoxene (0.7%)
B/L system III (125 ka)	No samples	No samples	Ilmenite + magnetite, tourmaline, epidote, staurolite, rutile, zircon, SKA, garnet, chromite + spinels	No samples	No samples
B/L system II (230 ka)	No samples	No samples	Ilmenite + magnetite, tourmaline, staurolite, rutile, zircon, SKA, garnet, chromite + spinels	No samples	No samples
B/L system I (325 ka)	No samples	No samples	Ilmenite + magnetite, zircon, staurolite, tourmaline, rutile, SKA, chromite, garnet, spinels	No samples	No samples

The composition and concentration of HMs, however, are not sufficient conditions to give rise to a mineral deposit. An economic mineral deposit depends on the existence of high-grade HMs concentration in a large volume of material; other way, one has an uneconomic HM occurrence. Then, it is to be discussed what kind of conditions led to the development of the Bujuru and Retiro HM deposits.

The deformational structures and the associated mechanical subsidence presented here must have played an important role in HM concentration and purification processes. But the deformational structures have definitively contributed to HMs concentration in a large volume of TD and TDS sediments. **Figure 12** shows a simplified geologic-structural sketch depicting the stratigraphic units distinguished by [25] and detailed in this work. **Figure 13** presents a synthesis of HM concentration, purification, and accumulation in different stages of structural development.

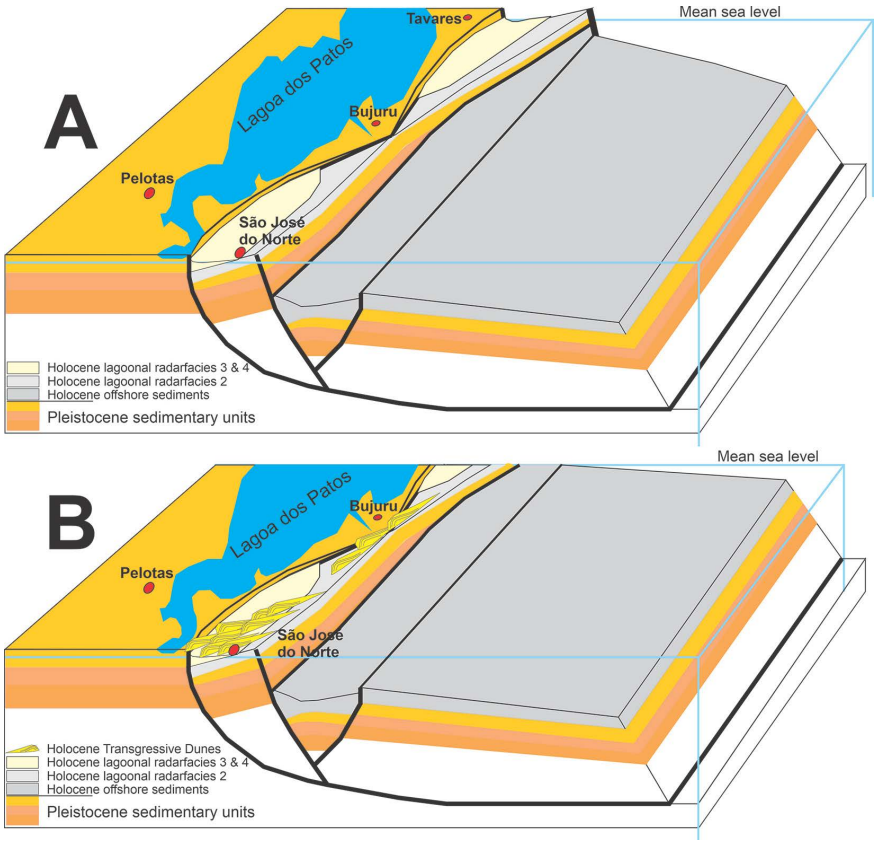

Figure 12. Geologic-structural model for placer Bujuru and Retiro HM deposits (RGSCP, Brazil). A) The development of the structural trap (placer) for the first stage of HM concentration. B) The third stage HM concentration and purification on Transgressive Dunes.

The first stage is characterized by a fault displacement rate higher than sedimentation rate and the development of a structural basin to constitute the main trap (placer) for preliminary HM concentration. The Pleistocene sedimentary unit rotation in the hanging-wall of listric normal fault developed a structural barrier

oceanward, whose remnants are still observed in recent beach line (e.g. [6]).

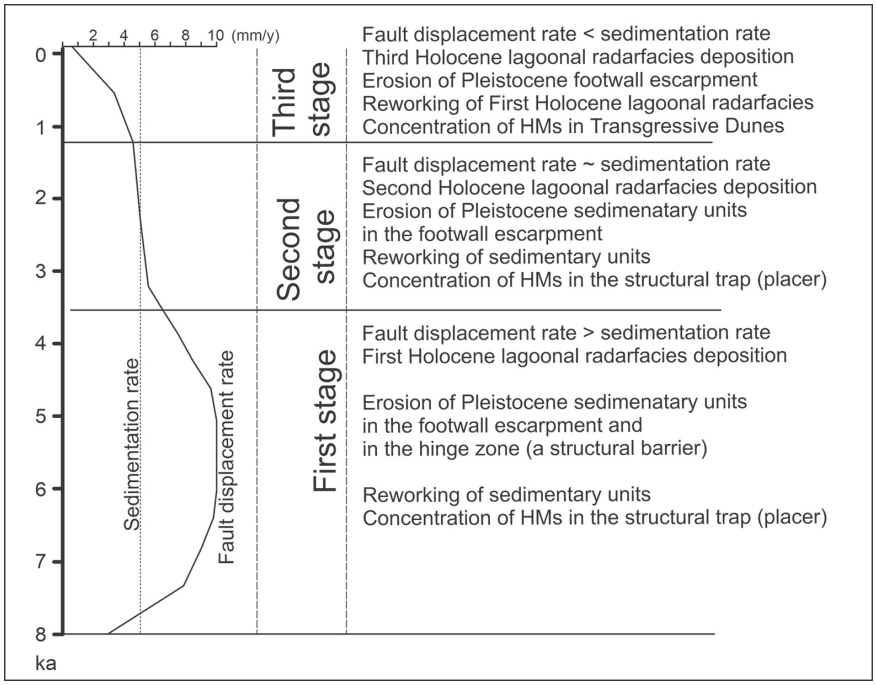

Figure 13. Diagram showing the development stages for structurally controlled lagoons, and the formation of Bujuru and Retiro HM deposits. Rate scale is only for illustration.

The erosion of that uplifted structural barrier was responsible for sediment reworking and deposition in the rapidly subsiding, fault-controlled lagoon (Lagoa do Peixe and Retiro-Estreito lagoons). Swash and backwash by waves and tides may have acted to erode Pleistocene units and to concentrate the HM in the First Lagoonal radarfacies (**Figure 12(A)**). The erosional process supported by the structural barrier was certainly facilitated by transfer faults, which open channels to ocean water sheets spreading on lagoons. These processes additionally contributed to HM concentration in the First Lagoonal radarfacies.

The second stage began in the period when fault displacement rate equals sedimentation rate (~3.46 ka upper age for the first lagoonal radarfacies). The corresponding radarfacies is not actual exposed, since it was deposited as a triangular unit (**Figure 12(A)**) in the asymmetric lagoon depocenter close to the fault escarpment [25]. This triangular zone was progressively developed during the high fault displacement and filled with sediments chiefly derived from Pleistocene footwall block (bulkhead structure west of fault). It also constitutes a structural trap for HMs. The continuity of fault displacement and hanging-wall block rotation (high to medium rates) began the folding of the first lagoonal radarfacies into brachysynclines and brachyanticlines. The sedimentation gap (3.46 to 1.06 ka) identified close to Bujuru beach is the time interval for the second lagoonal radarfacies deposition [25].

The third stage is characterized by a sedimentation rate higher than fault displacement rate and imply lagoon clogging due to sediments derived from Pleistocene

bulkhead (footwall structural high) to the west and from brachyanticline that was exposed near the beach. The peat layer (~1.06 ka) now exposed by folding in the beach is the lowermost strata of this radarfacies (4). At this stage, the initial Pleistocene structural barrier at the beach was completely eroded, and a new structural barrier is present: the brachyanticline. Tides and waves erosion on the previous lagoonal radarfacies exposed in the beach zones, HM hydraulic sorting in the offshore to backshore zones, onshore winds transport, and winnowing are the processes responsible for the Bujuru and Retiro HM deposits. The brachyanticline erosion and sediment transport by onshore winds are the main mechanisms building up the TDS and TD that are actually clogging the Lagoa do Peixe and Retiro-Estreito lagoons and giving rise to HM deposits (**Figure 12(B)**).

7. Conclusions

The RGSCP was developed close to a super-mature crustal section (RGS Precambrian Shield). The Bujuru and Retiro HM deposits were developed in a consequence of deformational traps (synthetic and antithetic normal faults). Mechanical subsidence and hanging-wall rotation due to gravitational tectonic, instead of sea level changes, are the main responsible for structural placers that lead to the existence of these HM deposits.

A three-stage evolutionary model is suggested based on fault displacement and sedimentation rates. A preliminary HM concentration episode was promoted by reworking sediments from the Pleistocene footwall escarpment and from a Pleistocene structural barrier developed in the hanging-wall oceanward. A second HM concentration episode is still in operation: TDS and TD developing upon another structural barrier (brachyanticline), that was build due to the progressive deformation of the hanging-wall upon the previous Holocene lagoonal radarfacies. The actual sedimentary barrier (TDS and TD) developed upon this brachyanticline barrier and migrates inland due to NE onshore winds, also accumulating over structurally controlled lagoons to clog them.

The results of this investigation seem to show a double evolution when classifying the aeolian landforms for Mostardas to Retiro-Estreito area in the RGSCP, following [24]. The structurally controlled Lagoa do Peixe and Retiro-Estreito lagoons, in the first and second stages of development, evolved as coastal lagoons (LFS 6), perennial lacustrine environment. The fine-grained sediments and organic matter define this depositional environment, as discussed in [25]. However, the third stage (recent) stage of development is now occurring as typical coastal-marine (LFS 5) in warm temperate climate and in microtidal-wave-dominated coastal-marine environments [22].

HM sources for this placer deposits seem to be regarded to Pleistocene sediments reworking induced by deformational structures. However, new HM input could have played an important role, chiefly due to longshore Atlantic currents as pointed out by [38].

HM transport and accumulation differ from first to second episodes. But,

erosion of previous Holocene lagoonal deposit, HM longshore transport, hydraulic sorting in the offshore to backshore zones, onshore winds transport, and winnowing are the envisaged processes as sedimentary structures show. Purification and diagenetic processes may have played another role in the relative concentration and composition of the HM deposits, as demonstrated by [3] [4] [42]. However, this subject was not under the scope of this paper and may be addressed in future investigations.

Acknowledgements

Authors thank Profa. Angélica Cirolini (UFSM), Prof. Alexandre F. Bruch (UFPel) and Prof. Christian Garcia Serpa (FURG) for DGPS support during geophysical surveys. B.S.F. also thanks to CNPq (Conselho Nacional de Desenvolvimento Científico e Tecnológico) for Doctoral grant. Authors thank Dr. Harald G. Dill (Gottfried Wilhelm Leibniz University, Hannover, Germany) for detailed revision and comments that improved the initial manuscript.

Conflicts of Interest

The authors declare no conflicts of interest regarding the publication of this paper.

References

[1] Hou, B., Keeling, J. and Van Gosen, B.S. (2017) Geological and Exploration Models of Beach Placer Deposits, Integrated from Case-Studies of Southern Australia. *Ore Geology Reviews*, **80**, 437-459. https://doi.org/10.1016/j.oregeorev.2016.07.016

[2] Nguyen, H.H., Carter, A., Hoang, L.V. and Vu, S.T. (2018) Provenance, Routing and Weathering History of Heavy Minerals from Coastal Placer Deposits of Southern Vietnam. *Sedimentary Geology*, **373**, 228-238. https://doi.org/10.1016/j.sedgeo.2018.06.008

[3] Dill, H.G., Kus, J., Kaufhold, S., Rammlmair, D. and Techmer, A. (2017) Oligo-Miocene Coal in a Microtidal Environment Reworked under Quaternary Periglacial Conditions (Western Falkland Islands/Isla Gran Malvina)—Coal Formation and Natural Sand Processing. *International Journal of Coal Geology*, **174**, 8-22. https://doi.org/10.1016/j.coal.2017.03.006

[4] Dill, H.G., Goldmann, S. and Cravero, F. (2018) Zr-Ti-Fe Placers along the Coast of NE Argentina: Provenance Analysis and Ore Guide for the Metallogenesis in the South Atlantic Ocean. *Ore Geology Reviews*, **95**, 131-160. https://doi.org/10.1016/j.oregeorev.2018.02.025

[5] Seck, M., Faye, S., Robertson, M. and Rose, M. (2018) Recycling Tailings Seepage Water for Diogo Heavy Minerals Mine Sustainability (Northern Senegal). *Journal of Water Resource and Protection*, **10**, 121-144. https://doi.org/10.4236/jwarp.2018.101008

[6] Dillenburg, S.R., Tomazelli, L.J. and Barboza, E.G. (2004) Barrier Evolution and Placer Formation at Bujuru Southern Brazil. *Marine Geology*, **203**, 43-56. https://doi.org/10.1016/s0025-3227(03)00330-x

[7] Aguiar Neto, A.B. (2015) Ocorrências de minerais pesados na Plataforma Continental

Interna/Média Oeste do Ceará. Doctoral Thesis, Universidade Federal do Ceará.

[8] França, P.P.D., Valença, L.M.M. and Souza Neto, J.A.D. (2013) Caracterização de minerais pesados e avaliação da radioatividade natural em sedimentos praiais de Acaú, Carne de Vaca e Ponta de Pedras, litoral norte do estado de Pernambuco. *Estudos Geológicos*, **23**, 37-51. https://doi.org/10.18190/1980-8208/estudosgeologicos.v23n1p37-51

[9] Sousa, S.S.D.C.G., Castro, J.W.D.A. and Guedes, E. (2017) Variações Granulométricas E Minerais Pesados Das Praias Do Norte Do Estado Do Rio de Janeiro, Se, Brasil: Condições de Distribuição E Deposição Dos Sedimentos. *Geosciences*, **36**, 365-380. https://doi.org/10.5016/geociencias.v36i2.12418

[10] Tomazzoli, E.R., Oliveira, U.R.d. and Horn Filho, N.O. (2007) Proveniência dos minerais de óxidos de Fe-Ti nas areias da praia do Pântano do Sul, ilha de Santa Catarina (SC), sul do Brasil. *Revista Brasileira de Geofísica*, **25**, 49-64. https://doi.org/10.1590/s0102-261x2007000500006

[11] Villwock, J.A., Loss, E.L., Dehnhardt, E.A., Tomazelli, L.J. and Hoffmeister, T. (1979) Concentraciones de arenas negras a lo largo de la costa de Rio Grande do Sul. Memorias del Seminario sobre ecologia bentônica y sedimentacion de la plataforma continental del Atlantico Sur. *Montevideo*, 407-414.

[12] Angelelli, V. and Chaar, E. (1967) Los depósitos de titanomagnetita, ilmenita e zircon de la Bahía San Blas (Tramo Baliza la Ballena-Faro segunda barranca), Partido Carmen de Patagones, Provincia de Buenos Aires. Informe 210, Comisión Nacional de Energía Atómica, República de Argentina.

[13] Cábana, M.C. and Mykietiuk, K. (1999) Arenas ferrotitaníferas y circoníferas del litoral de la provincia de Buenos Aires. In: *Recursos Minerales de la República Argentina*, Instituto de Geología y Recursos Minerales SEGEMAR, Buenos Aires (AR), 1899-1903.

[14] Isla, F.I. (1991) Spatial and Temporal Distribution of Beach Heavy Minerals: Mar Chiquita, Argentina. *Ocean and Shoreline Management*, **16**, 161-173. https://doi.org/10.1016/0951-8312(91)90002-j

[15] Ferreira, K.R.S. (2006) Caracterização do concentrado de Ilmenita produzido na Mina do Guaju, Paraíba, visando identificar inclusões de Monazita e outros contaminantes. Master Degree Dissertation, Universidade Federal do Rio Grande do Sul.

[16] Munaro, P. (1994) Geologia e Mineralogia do depósito de minerais pesados de Bujuru-RS. Master Degree Dissertation, Universidade Federal do Rio Grande do Sul.

[17] Slingerland, R.L. (1977) The Effects of Entrainment on the Hydraulic Equivalence Relationships of Light and Heavy Minerals in Sands. *SEPM Journal of Sedimentary Research*, **47**, 753-770. https://doi.org/10.1306/212f7243-2b24-11d7-8648000102c1865d

[18] Komar, P.D. and Wang, C. (1984) Processes of Selective Grain Transport and the Formation of Placers on Beaches. *The Journal of Geology*, **92**, 637-655. https://doi.org/10.1086/628903

[19] Patyk-Kara, N.G. (2002) Placers in the System of Sedimentogenesis. *Lithology and Mineral Resources*, **37**, 429-441. https://doi.org/10.1023/a:1020268115823

[20] Lalomov, A.V. (2003) Differentiation of Heavy Minerals in the Alongshore Debris Flow and Modeling of Processes of Coastal-Marine Placer Formation. *Lithology and Mineral Resources*, **38**, 306-313. https://doi.org/10.1023/a:1024607628886

[21] Roy, P.S. (1999) Heavy Mineral Beach Placers in Southeastern Australia; Their Nature and Genesis. *Economic Geology*, **94**, 567-588. https://doi.org/10.2113/gsecongeo.94.4.567

[22] Dill Harald, G. and Andrei, B. (2022) From the Aeolian Landform to the Aeolian Mineral Deposit in the Present and Its Use as an Ore Guide in the Past. Constraints from Mineralogy, Chemistry and Sediment Petrography. *Ore Geology Reviews*, **141**, Article 104490. https://doi.org/10.1016/j.oregeorev.2021.104490

[23] Dill, H.G. (2018) Gems and Placers—A Genetic Relationship Par Excellence. *Minerals*, **8**, Article 470. https://doi.org/10.3390/min8100470

[24] Dill, H.G. (2022) Trends and Composition—A Sedimentological-Chemical-Mineralogical Approach to Constrain the Origin of Quaternary Deposits and Landforms—From a Review to a Manual. *Geosciences*, **12**, Article 24. https://doi.org/10.3390/geosciences12010024

[25] Fontoura, B.S.d., Strieder, A.J., Corrêa, I.C.S. and Mendes, P.R. (2024) Gravity-Driven Listric Growth Fault and Sedimentation in the Lagoa Do Peixe, Rio Grande Do Sul Coastal Plain, Brazil. *Open Journal of Geology*, **14**, 594-616. https://doi.org/10.4236/ojg.2024.144025

[26] Barboza, E.G., Rosa, M.L.C.C., Dillenburg, S.R. and Tomazelli, L.J. (2013) Preservation Potential of Foredunes in the Stratigraphic Record. *Journal of Coastal Research*, **165**, 1265-1270. https://doi.org/10.2112/si65-214.1

[27] Dillenburg, S.R., Barboza, E.G., Rosa, M.L.C.C., Caron, F. and Sawakuchi, A.O. (2017) The Complex Prograded Cassino Barrier in Southern Brazil: Geological and Morphological Evolution and Records of Climatic, Oceanographic and Sea-Level Changes in the Last 7–6 Ka. *Marine Geology*, **390**, 106-119. https://doi.org/10.1016/j.margeo.2017.06.007

[28] Tomazelli, L.J. and Villwock, J.A. (1996) Quaternary Geological Evolution of Rio Grande do Sul Coastal Plain, Southern Brazil. *Anais da Academia Brasileira Ciências*, **68**, 373-382.

[29] Tomazelli, L.J., Dillenburg, S.R. and Villwock, J.A. (2000) Late Quaternary Geological History of Rio Grange do Sul Coastal Plain, Southern Brazil. *Revista Brasileira de Geociências*, **30**, 474-476. https://doi.org/10.25249/0375-7536.2000303474476

[30] Rosa, M.L.C.d.C., Barboza, E.G., Abreu, V.d.S., Tomazelli, L.J. and Dillenburg, S.R. (2017) High-Frequency Sequences in the Quaternary of Pelotas Basin (Coastal Plain): A Record of Degradational Stacking as a Function of Longer-Term Base-Level Fall. *Brazilian Journal of Geology*, **47**, 183-207. https://doi.org/10.1590/2317-4889201720160138

[31] Takahashi, R. and Hartmann, F. (2014) Relatório de Impacto Ambiental (RIMA) do Projeto Retiro (São José do Norte, RS, Brasil). CPEA—Consultoria, Planejamento e Estudos Ambientais Ltda. e HAR Engenharia e Meio Ambiente Ltda. Relatório Técnico apresentado ao IBAMA.

[32] Tomazelli, L.J. (1978) Minerais pesados da Plataforma Continental do Rio Grande do Sul. *Acta Geologica Leopoldensia*, **2**, 103-135.

[33] Barros, C.E.d., Nardi, L.V.S., Dillenburg, S.R., Baitelli, R. and Dehnhardt, B.A. (2008) Distribuição e origem dos minerais detríticos pesados das areias praiais holocênicas do litoral norte do Rio Grande do Sul. *Revista Brasileira de Geociências*, **38**, 319-335. https://doi.org/10.25249/0375-7536.2008382319335

[34] de Barros, C.E., Nardi, L.V.S., Dillenburg, S.R., Ayup, R., Jarvis, K. and Baitelli, R. (2010) Detrital Minerals of Modern Beach Sediments in Southern Brazil: A Provenance Study Based on the Chemistry of Zircon. *Journal of Coastal Research*, **261**, 80-93. https://doi.org/10.2112/06-0817.1

[35] Weschenfelder, J., Medeanic, S., Corrêa, I.C.S. and Aliotta, S. (2008) Holocene

Paleoinlet of the Bojuru Region, Lagoa Dos Patos, Southern Brazil. *Journal of Coastal Research*, **1**, 99-109. https://doi.org/10.2112/04-0369.1

[36] Jaboyedoff, M., Penna, I., Pedrazzini, A., Baroň, I. and Crosta, G.B. (2013) An Introductory Review on Gravitational-Deformation Induced Structures, Fabrics and Modeling. *Tectonophysics*, **605**, 1-12. https://doi.org/10.1016/j.tecto.2013.06.027

[37] Da Silva, M.A.M. (1979) Provenance of Heavy Minerals in Beach Sands, Southeastern Brazil: From Rio Grande to Chui (rio Grande Do Sul State). *Sedimentary Geology*, **24**, 133-148. https://doi.org/10.1016/0037-0738(79)90033-2

[38] Corrêa, I.C.S., Zouain, R.N.A., Weschenfelder, J. and Tomazelli, L.J. (2008) Áreas Fontes dos Minerais Pesados e sua Distribuição sobre a Plataforma Continental Sul-brasileira, Uruguaia e Norte-argentina. *Pesquisas em Geociências*, **35**, 137-150. https://doi.org/10.22456/1807-9806.17899

[39] Martins, L.P. (2011) Estudo e Avaliação das Assembléias de Minerais Pesados Detríticos das Areias Holocênicas Praiais da Margem Emersa da Bacia de Pelotas. Master Degree Dissertation, Universidade Federal do Rio Grande do Sul.

[40] Anoni, R.A.O. (2015) Estudo comparativo da assembleia de Minerias Pesados detríticos não-opacos dos depósitos praiais nos três sistemas Laguna-Barreira da porção extremo sul da Planície Costeira do Rio Grande do Sul. Geology Bachelor dissertation, Universidade Federal do Rio Grande do Sul.

[41] Carassai, J.J., Lavina, E.L.C., Junior, F.C. and Girelli, T.J. (2019) Provenance of Heavy Minerals for the Quaternary Coastal Plain of Southernmost Brazil (rio Grande Do Sul State). *Journal of Coastal Research*, **35**, 295-304. https://doi.org/10.2112/jcoastres-d-18-00066.1

[42] Dill, H.G. and Skoda, R. (2017) Provenance Analysis of Heavy Minerals in Beach Sands (Falkland Islands/Islas Malvinas)—A View to Mineral Deposits and the Geodynamics of the South Atlantic Ocean. *Journal of South American Earth Sciences*, **78**, 17-37. https://doi.org/10.1016/j.jsames.2017.06.005